R. & M. No. 2642
(11,562, 11,694)
A.R.C. Technical Report

MINISTRY OF SUPPLY

AERONAUTICAL RESEARCH COUNCIL
REPORTS AND MEMORANDA

The Induced Velocity Field of a Rotor

By

K. W. MANGLER and H. B. SQUIRE

LONDON: HER MAJESTY'S STATIONERY OFFICE
1953
FIVE SHILLINGS NET

The Induced Velocity Field of a Rotor

By

K. W. MANGLER and H. B. SQUIRE

COMMUNICATED BY THE PRINCIPAL DIRECTOR OF SCIENTIFIC RESEARCH (AIR), MINISTRY OF SUPPLY

*Reports and Memoranda No. 2642**

May, 1950

Summary.—A short account and the results of a theoretical investigation (*cf.* Ref. 1 and 2) of the velocity field induced by a lifting rotor is given. The computation is based on the assumptions that the rotor is lightly loaded and that it has an infinite number of blades. This is applied to calculate the induced velocity distribution for disc incidences of 0, 15, 30, 45 and 90 deg. For the downwash at the rotor itself (the normal component of the induced velocity) the Fourier coefficients are given, as they are needed for the calculation of the blade motion.

1. *Introduction.*—The velocity field, which is induced by a lifting rotor, is of interest in connection with its effect on the blade motion and on a neighbouring rotor or other body. In its general form the calculation of this velocity field is extremely complicated, and it would be impracticable to derive useful results without introducing a number of simplifying assumptions.

Since hitherto nothing better was available, it has been assumed by most authors, following Glauert, that the induced velocity is constant over the disc. Glauert also considered the effect of a downwash which is linearly distributed from front to rear of the disc. Coleman and others[3] have calculated the downwash for a uniformly loaded circular disc, assuming that the wake has the shape of an elliptic cylinder. They actually derive only the mean value of the induced velocity along the fore-and-aft diameter of the disc and the derivative in the middle of the disc in that direction.

The present investigation is an attempt to provide a method of calculation of the induced velocity distribution, which involves only acceptable assumptions. The principal one of these is the assumption of an infinite number of blades, so that the rotor can be replaced by a circular disc with a pressure step between its faces. This is permissible as long as the angular velocity of the blades is sufficiently high. The second main assumption is that the disc is only lightly loaded, or that the stream velocity is not too small, so that the induced velocities are everywhere small compared to the stream velocity. This assumption is usual in investigations of the present type, as long as one is not interested in the conditions of the hovering rotor, and enable us to employ the linearized theory as it is explained, *e.g.*, in Durand, Vol. 2, by Burgers[4]. On the other hand it implies a serious limitation in the applicability of the results. The various less important assumptions which have been made, *e.g.*, the neglect of the induced velocities associated with the rotor torque, will become apparent during the course of the investigation.

The present report gives a brief discussion of the investigations and the results of the calculations of the induced velocity distributions. A detailed description of the method of calculation is given in Ref. 1 and 2.

* Summary report of R.A.E. Report No. Aero. 2247 (A.R.C. 11562) and R.A.E. Tech. Note No. 1958 (A.R.C. 11694), 1948.

2. *The Velocity Field of a Rotor.*—We replace the helicopter rotor by a circular disc with a thrust T distributed over it. The thrust is everywhere normal to the disc and is equivalent to a discontinuity in pressure between the two faces of the disc. The small forces in the plane of the disc, which corresponds to the torque distribution, are neglected. The axes and notation are shown in Fig. 1. The undisturbed flow of the velocity V is directed opposite to the positive x-axis and the disc is inclined at an angle i. We denote the components of the additional velocity vector $\underline{v}$ which is caused by the helicopter thrust, by u, v, w. It is assumed that these velocities are small compared with the stream velocity V. This condition is satisfied, if the thrust coefficient

$$C_T = \frac{T}{\pi R^2 . \frac{1}{2}\rho V^2} \quad \ldots \ldots \ldots \ldots \ldots \ldots \ldots \ldots \quad (1)$$

($2R$ = diameter of the rotor, T = overall thrust, ρ = air density)
is small compared to 1. Then the Euler equations can be simplified in such a way that only linear terms are retained:

$$-V\frac{\partial \underline{v}}{\partial x} = -\frac{1}{\rho}\operatorname{grad} p \quad \ldots \ldots \ldots \ldots \ldots \ldots \ldots \quad (2)$$

where p is the static pressure. Since the continuity equation

$$\operatorname{div} \underline{v} = 0 \quad \ldots \ldots \ldots \ldots \ldots \ldots \ldots \quad (3)$$

must also be satisfied, it follows from equations (2) and (3) that

$$\operatorname{div}\operatorname{grad} p = \nabla^2 p = 0. \quad \ldots \ldots \ldots \ldots \ldots \ldots \quad (4)$$

Therefore p is a potential function, which satisfies Laplace's equation (4), and the acceleration $-V\,\partial \underline{v}/\partial x$ is obtained as the gradient of this potential function according to equation (2). So we obtain by integrating equation (2)

$$\frac{\underline{v}}{V} = \frac{1}{\rho V^2}\int_{+\infty}^{x} \operatorname{grad} p \, dx . \quad \ldots \ldots \ldots \ldots \ldots \quad (5)$$

Here the lower limit of the integration is $+\infty$, because the induced velocity $\underline{v}$ vanishes far ahead of the rotor. This result equation (5) applies everywhere outside the wake, which is bounded by straight lines, extending downstream from the edge of the rotor disc and parallel to the undisturbed velocity.

Inside the wake a special investigation is necessary. We note first that the induced velocity must be continuous across the disc. This is true for the component normal to the disc for continuity reasons. It is also necessary for the components parallel to the disc, because a discontinuity would mean the existence of forces in the plane of the disc (*e.g.*, torque forces), which, however, have been assumed to be absent. Thus we may use equation (5) to determine the induced velocity everywhere provided that for points in the wake we make the induced velocity continuous across the disc. As a consequence of this we obtained a flow that contains vorticity inside the wake. For the velocity component parallel to the wind direction, equation (5) gives

$$\frac{u}{V} = \frac{p - p_\infty}{\rho V^2} \text{ outside the wake} \quad \ldots \ldots \ldots \ldots \quad (6)$$

and

$$\frac{u}{V} = \frac{(p - p_\infty) + (p_u - p_0)}{\rho V^2} \text{ inside the wake} \quad \ldots \ldots \ldots \quad (7)$$

where p_∞ is the pressure in the undisturbed flow and $(p_u - p_0)$ is the pressure rise across the disc directly ahead of the point under consideration.

The solution of the Laplace equation (4) is obtained following Kinner[5] in terms of Legendre functions of the elliptic co-ordinates associated with the disc, which are discontinuous between the two faces of the disc, but continuous everywhere else. It is then possible to determine the induced velocities by means of equation (5) for some simple types of load distribution $(p_u - p_0)$ over the disc, but even for these the integration in equation (5) is difficult and cumbersome.

The calculations were restricted to the case of an axially symmetrical load distribution so that the load depends only on the distance r' from the centre of the disc, but not on the azimuth angle ϕ. Any such distribution can be expanded in a series of the above mentioned Legendre functions, so that the first term produces the entire thrust T and the rest of the series produces only certain variations of the load distribution.

The first load distribution which was considered was an elliptic load distribution (the first term of this series)

$$\frac{p_u - p_0}{\rho V^2 C_T} = \frac{3}{4}\left(1 - \frac{r'^2}{R^2}\right)^{1/2} \quad \ldots \quad \text{(I)}$$

where C_T is the thrust coefficient defined in equation (1). The second term of this series gave the second pressure distribution (II), that was treated, but which is only useful as a step to the third pressure distribution;

$$\frac{p_u - p_0}{\rho V^2 C_T} = \frac{15}{8}\frac{r'^2}{R^2}\left(1 - \frac{r'^2}{R^2}\right)^{1/2} \quad \ldots \quad \text{(III)}$$

This is a linear combination of (I) and (II), chosen in such a way that the load vanishes at the edge and in the middle of the rotor, which may be a reasonable approximation for the load existing at a rotor in forward flight. These distributions are shown in Fig. 2. Having determined the induced velocity field for the load distributions (I) and (III) it is best to forget about the intermediate distribution (II). The distributions (I) and (III) can be regarded as basic and data for other related distributions can be obtained by linear combination of the results for (I) and (III).

3. *Results of the Calculation.*—The most significant components of the induced velocity are the component $\bar{w}$ normal to the disc at its surface, which is important for the blade motion, and the vertical component w far downstream, which is necessary, *e.g.*, for an estimation of the mutual influence of the rotors of a helicopter with several rotors. These functions $\bar{w}$ and w have been calculated for values of the incidence angle $i = 0$, 15, 30, 45 and 90 deg, as outlined and described in detail in Ref. 1.

The results of these calculations for the load distributions (I) and (III) are given in Figs. 3 to 12 in the form of contour lines of $\bar{w}/(VC_T)$ over the disc and in Figs. 13 to 20 in the form of contour lines of $w/(VC_T)$ over a plane normal to the stream direction and far downstream. (The results are also given in Tables 1 to 7 for $\bar{w}/(VC_T)$ and in Tables 8 to 14 for $w/(VC_T)$, in Ref. 1.) The downwash $\bar{w}$ at the disc can also be computed by means of the Fourier series, described in the section 4. For points near the edge of the rotor, the convergence of the Fourier series is not good and the tables of Ref. 1 should preferably be used.

As can be seen from the figures, the downwash distribution over the rotor disc is far from constant and depends very much upon the form of the pressure distribution. Local peaks in upwash, which occur on the sides of the disc, can be removed by fairly small alterations of the load distribution. Therefore, the peaks, calculated in some cases near the rim of the disc, may not occur in practice, and we take only the general features as significant.

The vertical component of the induced velocity far behind the rotor is directed downwards near the middle and upwards on both sides. The downwash is symmetrical with respect to the plane $z = 0$. At the boundary of the wake we have a singularity so that the contour lines have a discontinuity in slope there. It may be mentioned here that the induced velocity w at a point situated not too close to the rotor and inside the cone $z^2 + y^2 = x^2$ can be assessed by the following asymptotic expansion[1] :—

$$\frac{w}{VC_T} - \left(\frac{w}{VC_T}\right)_{x=\pm\infty} = \mp\frac{R^2}{8x^2}\left\{\frac{\cos i}{2} + \frac{z}{x}\sin i + \frac{M}{xT}\cos 2i + \cdots\right\} \quad \ldots \quad (8)$$

Here T is the overall thrust and M the pitching moment referred to a line passing through the centre of the disc. The equation can be used far ahead ($x > 0$) with the upper sign or far behind the rotor ($x < 0$) with the lower sign.

4. *Fourier Series Representation.*—The downwash distribution over the rotor disc may be important in connection with the calculation of the blade motion. For this purpose it is useful to represent the results in the form of a Fourier series :—

$$\frac{\bar{w}}{VC_T} = \frac{a_0(r',i)}{2} + \sum_{h=1}^{\infty} a_n(r',i) \cos n\phi. \quad .. \quad .. \quad .. \quad .. \quad .. \quad (9)$$

Here ϕ is the azimuth angle measured from the up-wind direction (Fig. 1) and r' the distance from the centre. Since only pressure distributions with lateral symmetry have been considered, only cosine-terms appear in the expansion (9).

The m-th coefficient is obtained by multiplying equation (9) by cos $m\phi$ and integrating it over ϕ between $-\pi$ and $+\pi$. The details of the method are explained in Ref. 2. The results are as follows :—

Load distribution (I) :—

The coefficients in the series (9) are denoted by a_{1n} in this case. Then we have with $\mu_0 = \left(1 - \frac{r'^2}{R^2}\right)^{1/2}$:

$$\left.\begin{aligned} a_{10} &= \tfrac{3}{4}\mu_0 = \frac{p_0 - p_u}{\rho V^2 C_T} = \frac{3}{4}\left(1 - \frac{r'^2}{R^2}\right)^{1/2} \\ a_{11} &= -\frac{3\pi}{16}(1-\mu_0^2)^{1/2}\left(\frac{1-\sin i}{1+\sin i}\right)^{1/2} \end{aligned}\right\} .. \quad .. \quad (10)$$

and for even values of $n \geqslant 2$

$$a_{1n} = (-1)^{(n-2)/2}\frac{3}{4}\left(\frac{n+\mu_0}{n^2-1}\right)\left(\frac{1-\mu_0}{1+\mu_0}\right)^{n/2}\left(\frac{1-\sin i}{1+\sin i}\right)^{n/2} \quad .. \quad .. \quad (11)$$

and for odd values of $n \geqslant 3$

$$a_{1n} = 0. \quad .. \quad .. \quad .. \quad .. \quad .. \quad .. \quad .. \quad .. \quad .. \quad (12)$$

Load Distribution (III) :—

Here the coefficients in series (9) are denoted by a_n. Then we have

$$\left.\begin{aligned} a_0 &= \tfrac{15}{8}\mu_0(1-\mu_0^2) = \frac{p_0 - p_u}{\rho V^2 C_T} \\ a_1 &= -\frac{15\pi}{256}(5 - 9\mu_0^2)(1-\mu_0^2)^{1/2}\left(\frac{1-\sin i}{1+\sin i}\right)^{1/2} \\ a_3 &= \frac{45\pi}{256}(1-\mu_0^2)^{3/2}\left(\frac{1-\sin i}{1+\sin i}\right)^{3/2} \end{aligned}\right\} .. \quad (13)$$

For even values of $n \geqslant 2$ we have

$$a_n = (-1)^{(n-2)/2}\frac{15}{8}\left[\frac{n+\mu_0}{n^2-1}\cdot\frac{9\mu_0^2 + n^2 - 6}{n^2-9} + \frac{3\mu_0}{n^2-9}\right]\left(\frac{1-\mu_0}{1+\mu_0}\right)^{n/2}\left(\frac{1-\sin i}{1+\sin i}\right)^{n/2} .. \quad (14)$$

and for odd values of $n \geqslant 5$

$$a_n = 0. \quad .. \quad .. \quad .. \quad .. \quad .. \quad .. \quad .. \quad .. \quad (15)$$

The first coefficient is always independent of the incidence angle i and proportional to the load distribution. The magnitude of the higher coefficients decreases fairly quickly due to the factor

$$\left(\frac{1-\mu_0}{1+\mu_0}\right)^{n/2}\left(\frac{1-\sin i}{1+\sin i}\right)^{n/2}.$$

So, apart from points near the rim of the disc at zero incidence, the Fourier series is very useful for determining the numerical values of the downwash distribution.

The mean value w' of the normal induced velocity over the whole disc is given by the integral

$$\frac{w'}{VC_T} = \frac{1}{\pi R^2}\int_{-\pi}^{\pi}\int_0^R \frac{\bar{w}}{VC_T} r'\, dr'\, d\phi. \quad \ldots \quad \ldots \quad \ldots \quad \ldots \quad \ldots \quad \ldots \quad (16)$$

Substituting from (9), equation (16) gives

$$\frac{w'}{VC_T} = \int_0^1 a_0 \frac{r'}{R} d\left(\frac{r'}{R}\right) = \int_0^1 a_{10} \frac{r'}{R}\, d\left(\frac{r'}{R}\right) = \frac{1}{4}; \quad \ldots \quad \ldots \quad \ldots \quad \ldots \quad (17)$$

for details *see* Refs. 1 and 2. Equation (17) is equivalent to the relation for the mean downwash over the disc of a rotor which was proposed by Glauert as a generalisation of the induced velocity formulae for an elliptically loaded wing and over the disc of a conventional propeller. Equation (17) is, however, restricted to lightly loaded rotors, whereas Glauert's formula is more general, though its validity has not yet been established.

5. *Notes on the Significance of the Results.*—The principal object of the investigation was to construct a sound mathematical theory for the induced velocity field of a rotor. This has been done within certain limitations, the principal ones being (1) the restriction to small disturbances, usual in aerofoil theory, and (2) the assumption of an infinite number of blades. There would be no fundamental difficulty in the extension of the theory to cover unsymmetrical load distributions such as occur in practice owing to the differences in flow at the advancing and at the retreating blade.

There is no satisfactory experimental check on the theory at present available. Measurements of the downwash behind a model rotor[6] showed that the theory agreed with experiment fairly well for the flow in the wake in some cases.

NOTATION

ρ	Air density
V	Free-stream velocity
i	Incidence of the rotor disc
R	Radius of the disc
p	Static pressure
$p_u - p_0$	Pressure rise across the disc
T	Thrust
C_T	Thrust coefficient $2T/\rho V^2 \pi R^2$
x, y, z	Rectangular Cartesian co-ordinates (Fig. 1), with x measured against the stream direction
x', y', z'	Alternative Cartesian co-ordinates (Fig. 1)
r', ϕ	Polar co-ordinates for points on the disc (Fig. 1)
$\underline{v}$	Vector of the induced velocities
u, v, w	Induced velocity components parallel to x, y, z
$\bar{w}, \bar{v}, \bar{w}$	Induced velocity components parallel to x', y', z'
a_n	Fourier coefficients (equation (9))
μ_0	$[1 - (r'/R)^2]^{1/2}$

REFERENCES

No.	*Author*	*Title, etc.*
1	K. W. Mangler	Calculation of the Induced Velocity Field of a Rotor. A.R.C. 11,562*. 1948. (Unpublished.)
2	K. W. Mangler	Fourier Coefficients for the Downwash at a Helicopter Rotor. A.R.C. 11,694*. 1948. (Unpublished.)
3	R. P. Coleman, A. M. Feingold and C. W. Stempin	Evaluation of the Induced Velocity Field of an Idealised Helicopter Rotor. N.A.C.A. A.R.R. No. L5E10. June, 1945.
4	Th. von Kármán and F. M. Burgers ..	Perfect Fluids. *Aerodynamic Theory*, Vol. 2. Ed. W. F. Durand. Berlin. 1935.
5	W. Kinner	Die kreisfoermige Tragflaeche auf potentialtheoretischer Grundlage. Theory of the Circular Wing. *Ingenieur Archiv.* Vol. 7, p. 47. 1937. Translated in R.T.P. Translation No. 2345, issued by the Ministry of Aircraft Production.
6	R. A. Fail and R. C. W. Eyre	Downwash Measurements behind a 12-ft diameter Helicopter Rotor in the 24-ft Wind Tunnel. A.R.C. 12,895. (To be published.)

* These have been re-written and are published as this Summary Report.

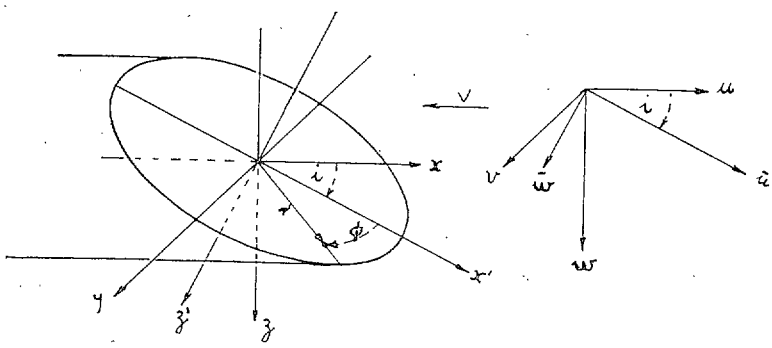

FIG. 1. Axes and notation.

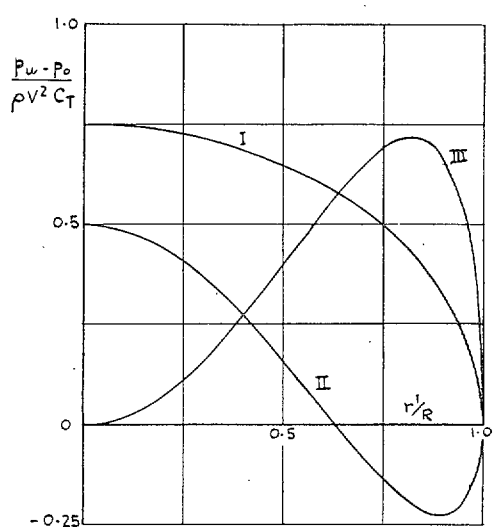

FIG. 2. Pressure distributions on the rotor disc.

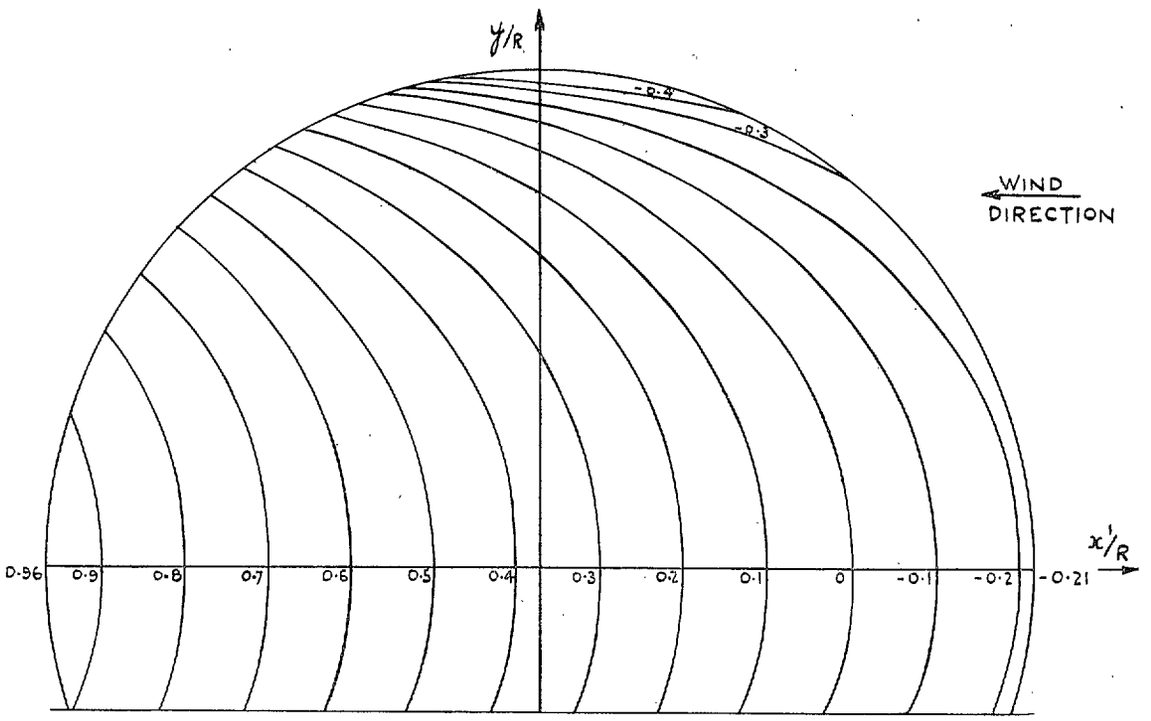

FIG. 3. Induced velocity over disc for pressure distribution (I). Contours of $\bar{w}/VC_T$ for $i = 0$ deg.

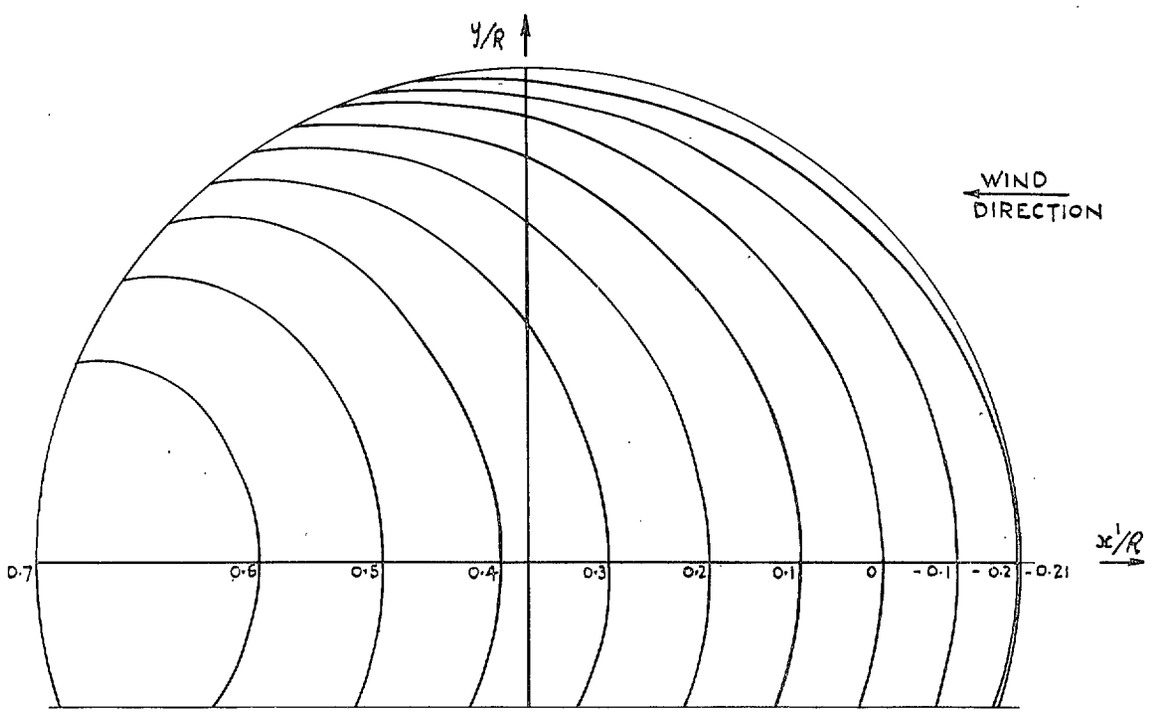

FIG. 4. Induced velocity over disc for pressure distribution (I). Contours of $\bar{w}/VC_T$ for $i = 15$ deg.

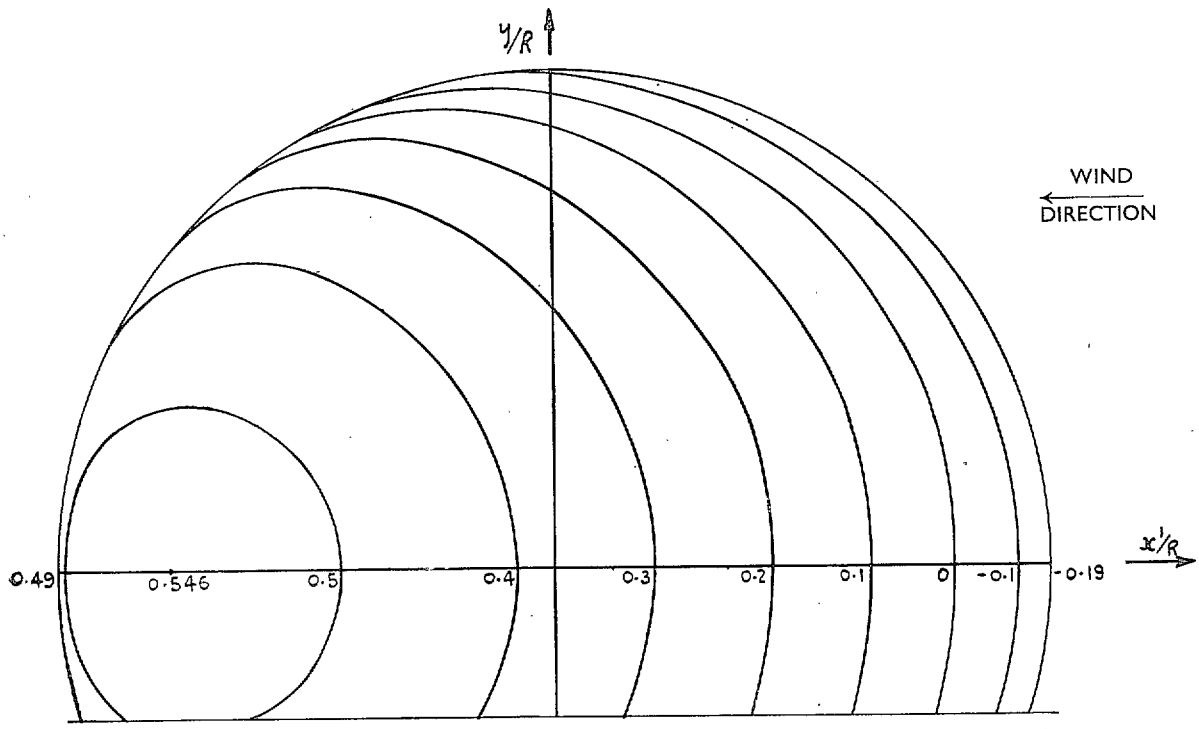

FIG. 5. Induced velocity over disc for pressure distribution (I). Contours of $\bar{w}/VC_T$ for $i = 30$ deg.

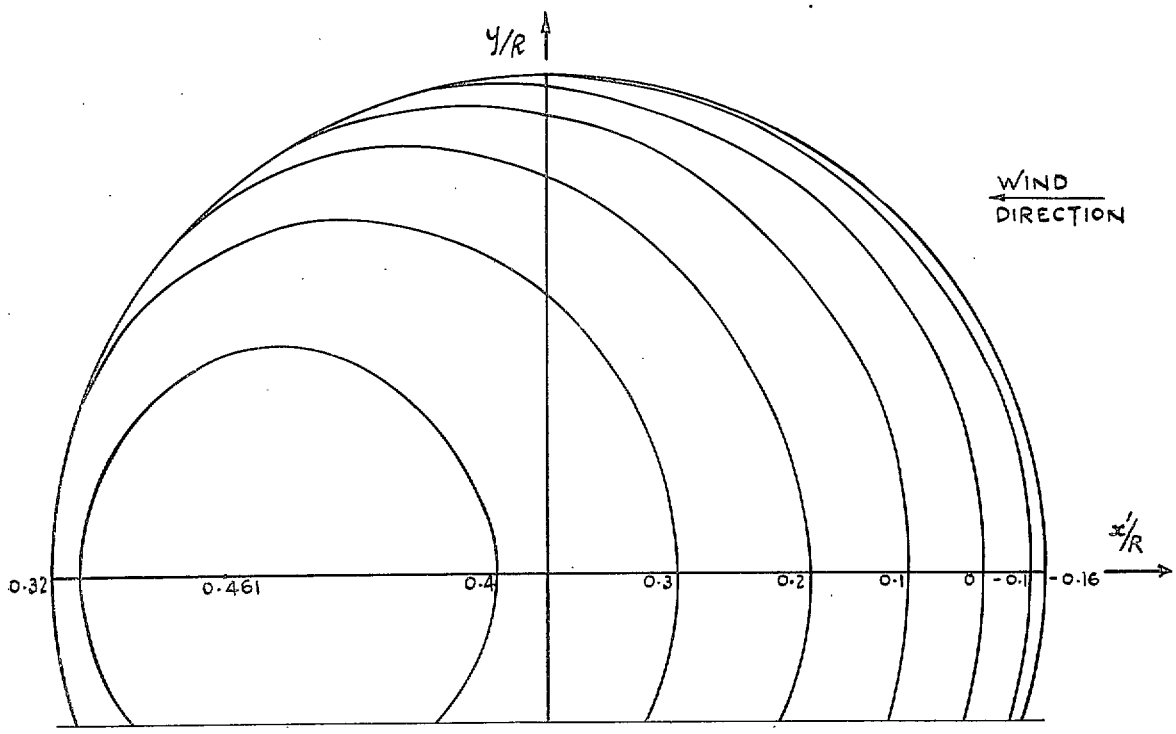

FIG. 6. Induced velocity over disc for pressure distribution (I). Contours of $\bar{w}/VC_T$ for $i = 45$ deg.

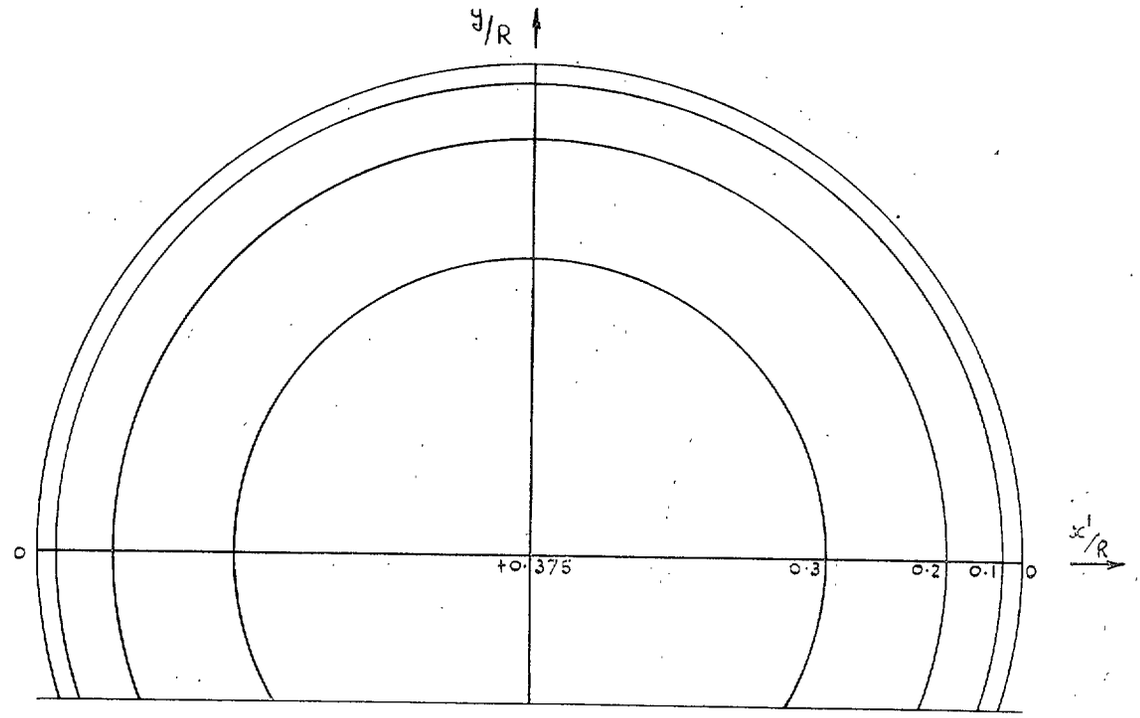

FIG. 7. Induced velocity over disc for pressure distribution (I). Contours of $\bar{w}/VC_T$ for $i = 90$ deg.

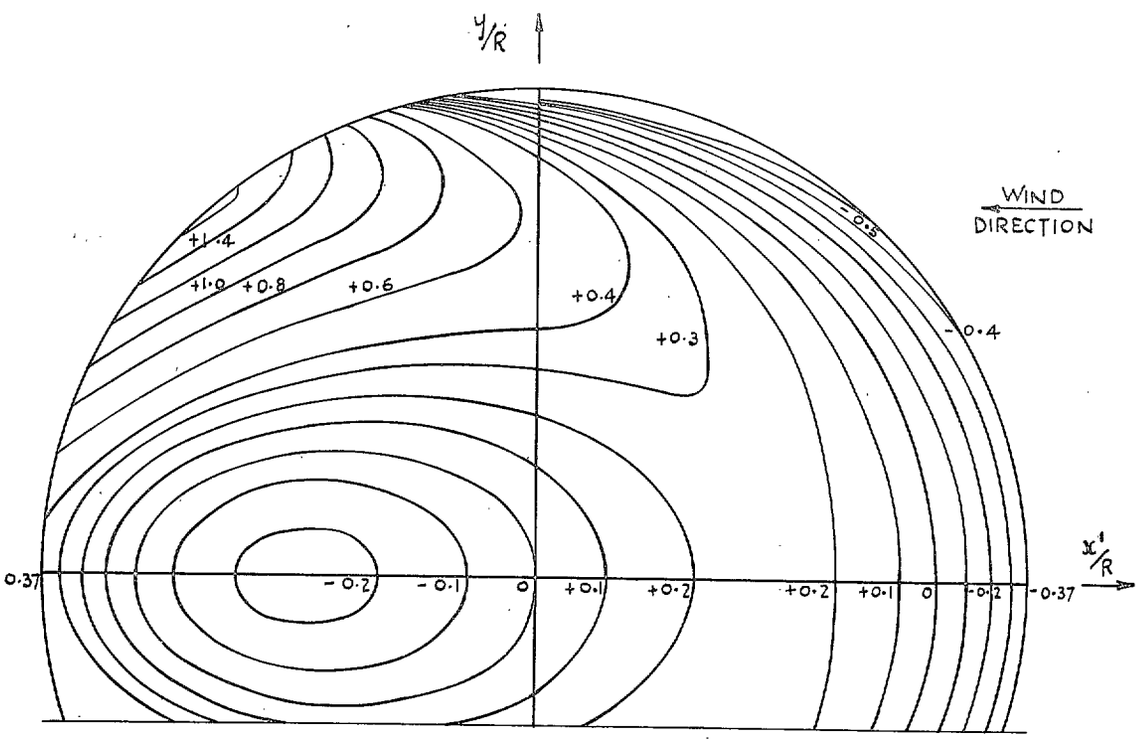

FIG. 8. Induced velocity over disc for pressure distribution (III). Contours of $\bar{w}/VC_T$ for $i = 0$ deg.

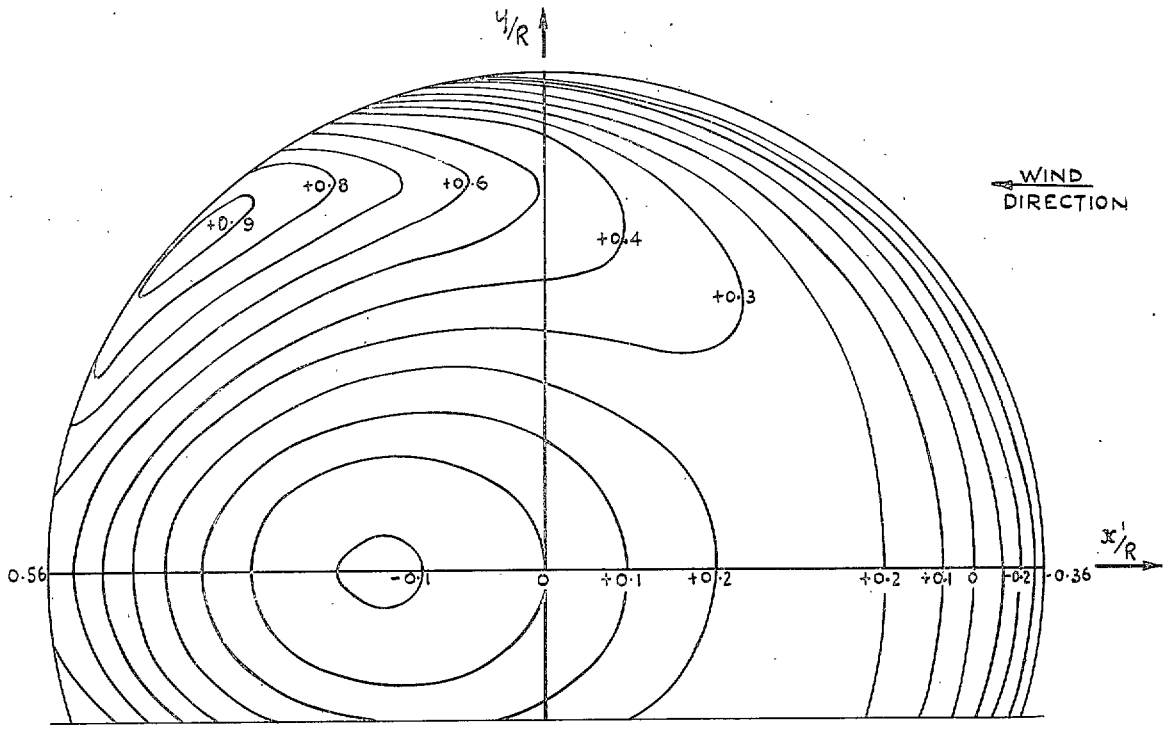

FIG. 9. Induced velocity over disc for pressure distribution (III). Contours of $\bar{w}/VC_T$ for $i = 15$ deg.

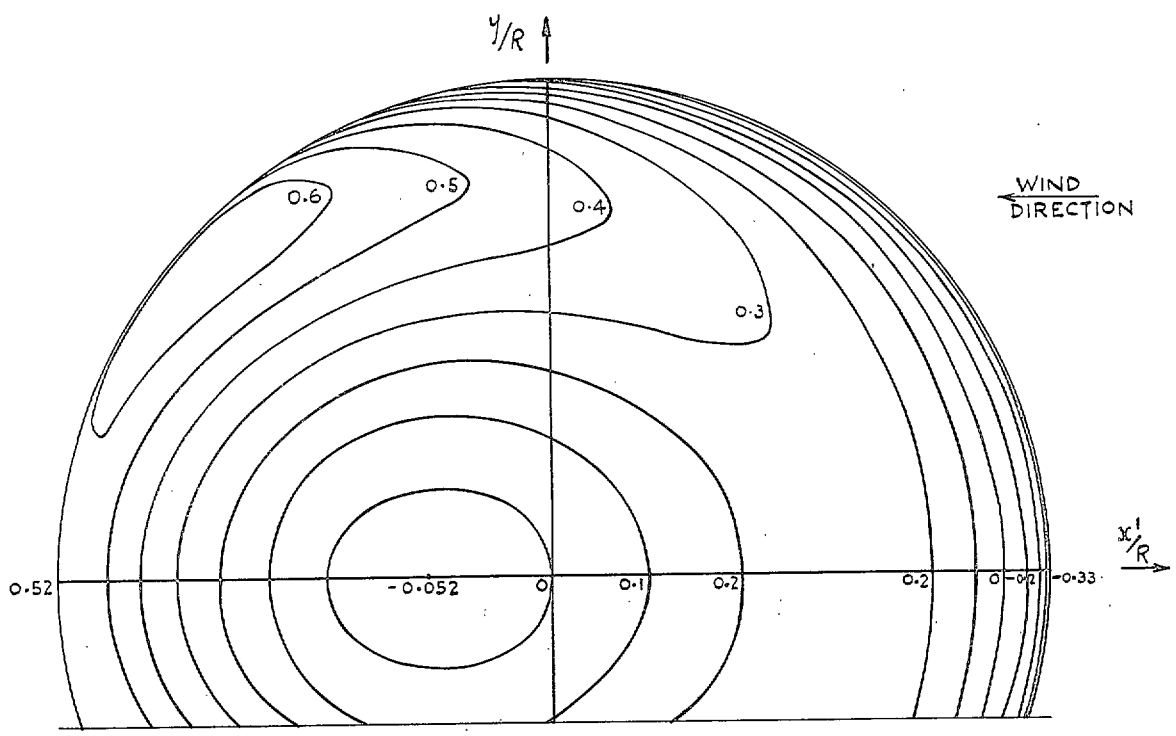

FIG. 10. Induced velocity over disc for pressure distribution (III). Contours of $\bar{w}/VC_T$ for $i = 30$ deg.

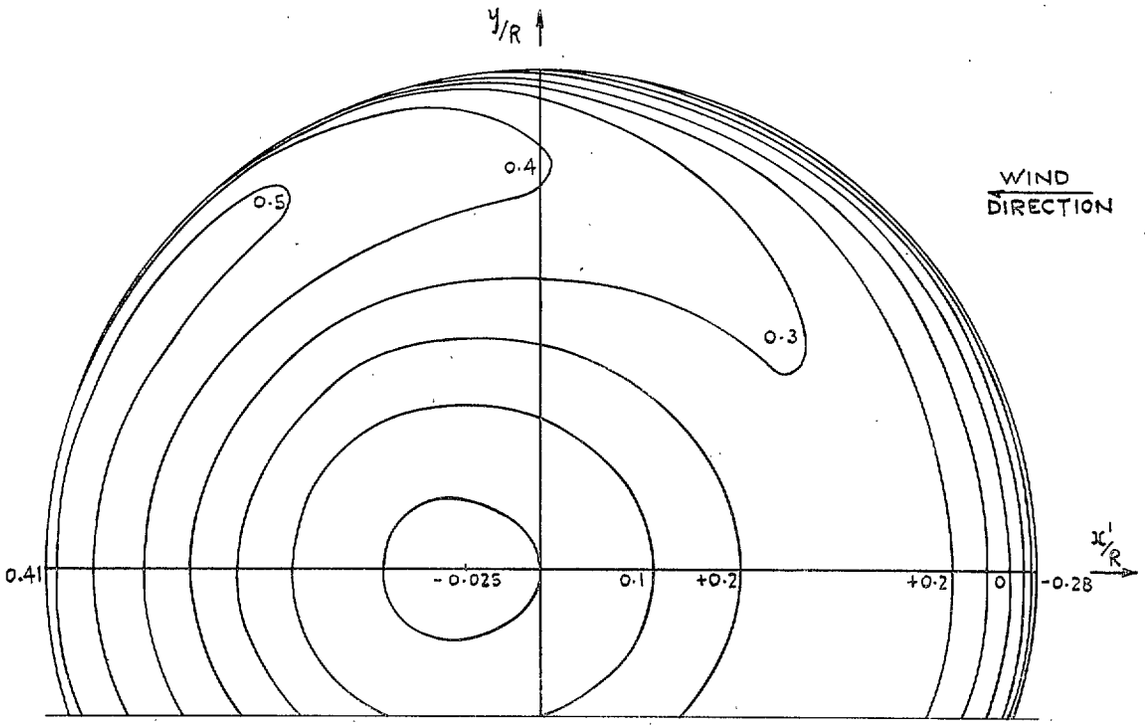

FIG. 11. Induced velocity over disc for pressure distribution (III). Contours of $\bar{w}/VC_T$ for $i = 45$ deg.

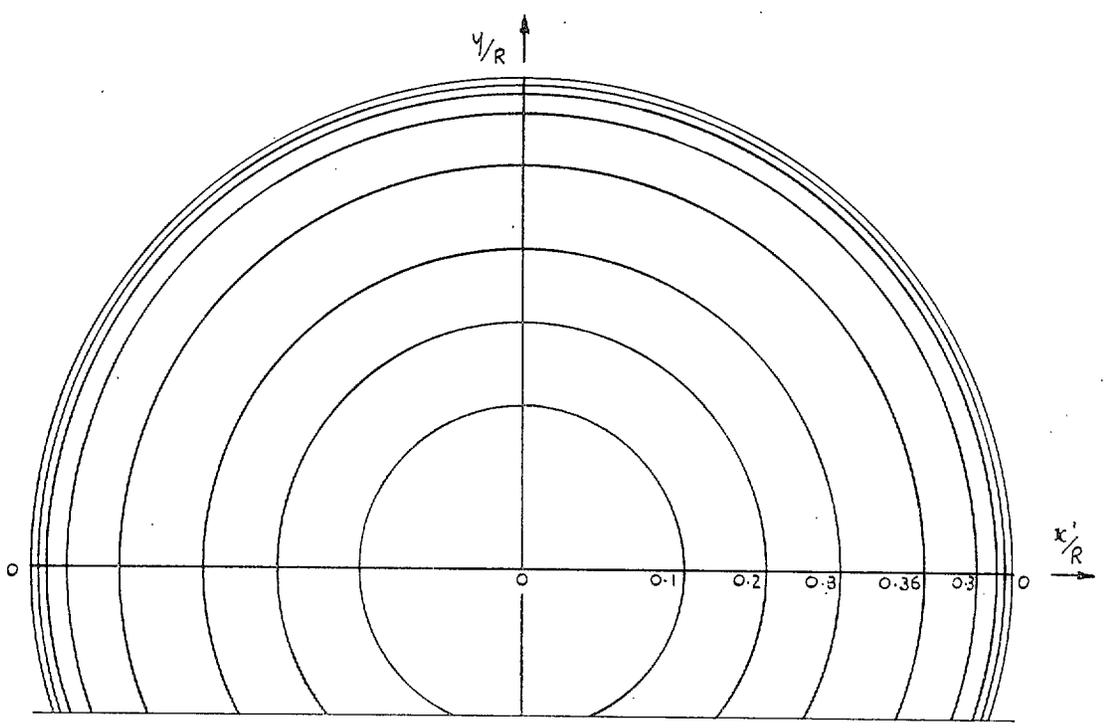

FIG. 12. Induced velocity over disc for pressure distribution (III). Contours of $\bar{w}/VC_T$ for $i = 90$ deg.

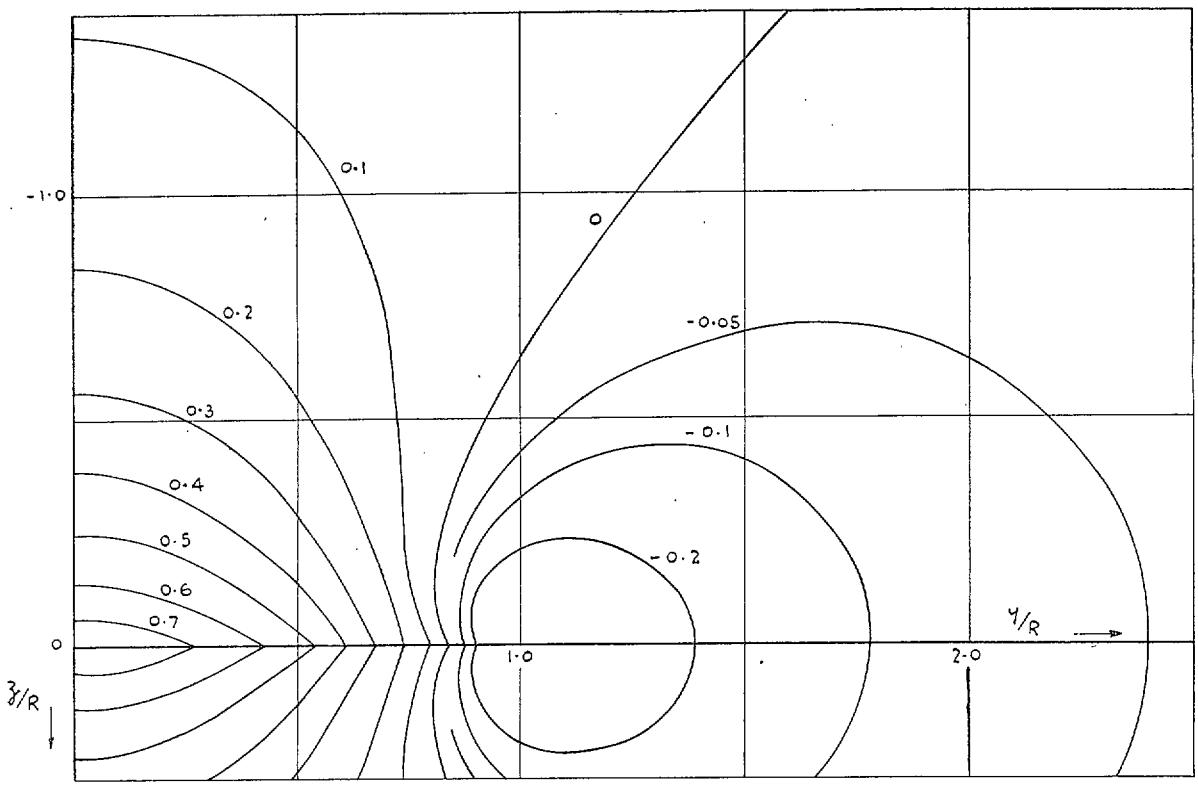

FIG. 13. Induced velocity far downstream for pressure distribution (I). Contours of w/VC_T for $i = 0$ deg.

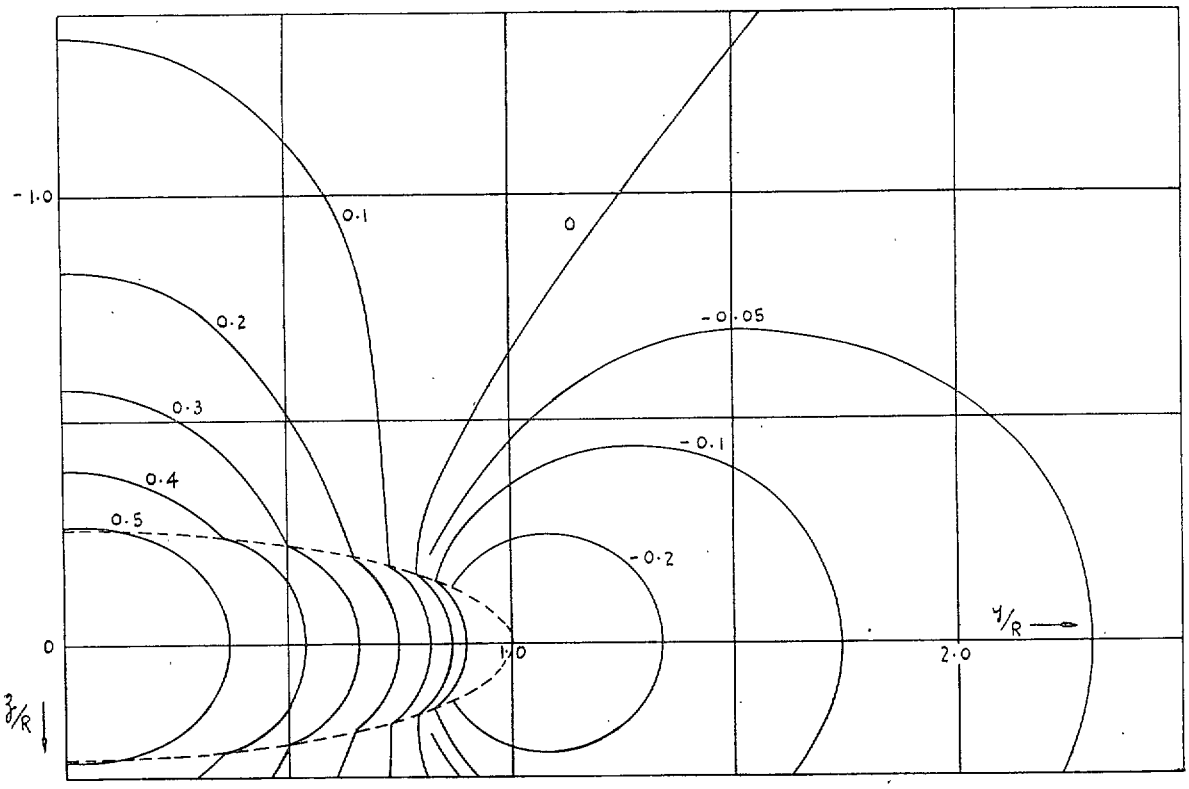

FIG. 14. Induced velocity far downstream for pressure distribution (I). Contours of $\bar{w}/VC_T$ for $i = 15$ deg.

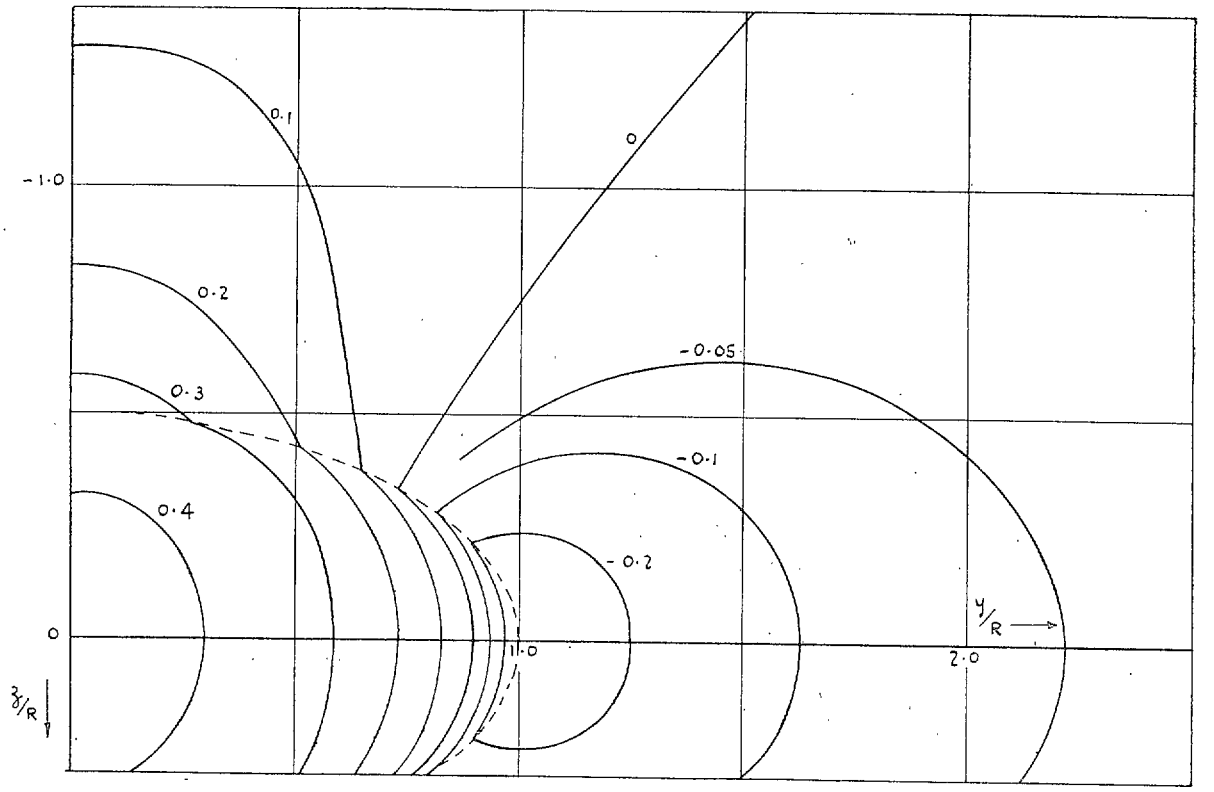

FIG. 15. Induced velocity far downstream for pressure distribution (I). Contours of w/VC_T for $i = 30$ deg.

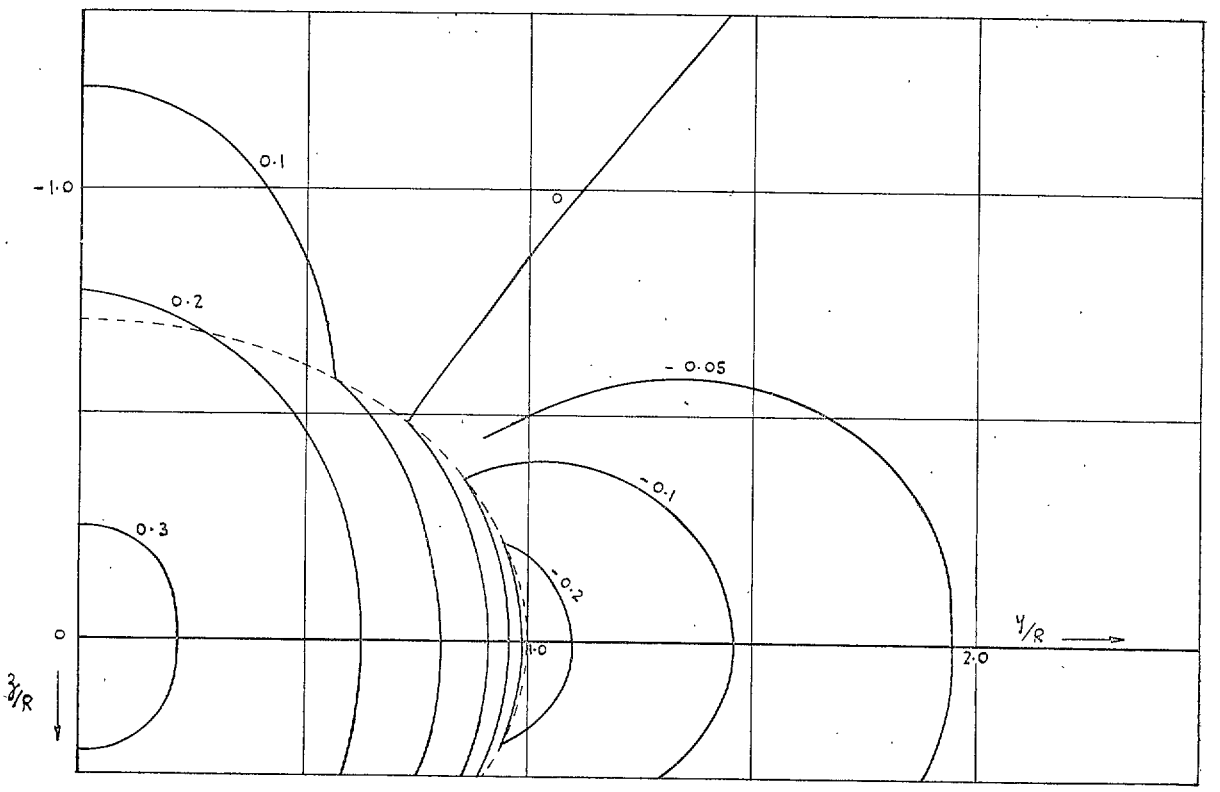

FIG. 16. Induced velocity far downstream for pressure distribution (I). Contours of w/VC_T for $i = 45$ deg.

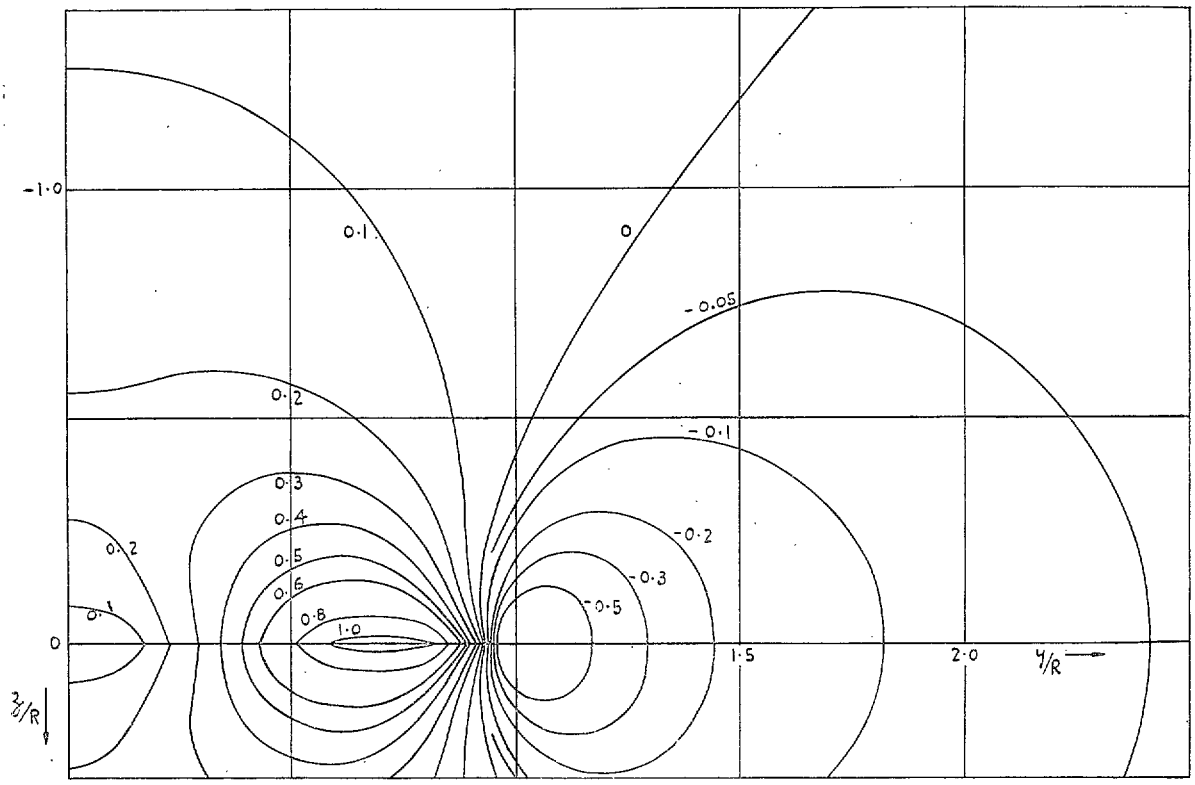

FIG. 17. Induced velocity far downstream for pressure distribution (III). Contours of w/VC_T for $i = 0$ deg.

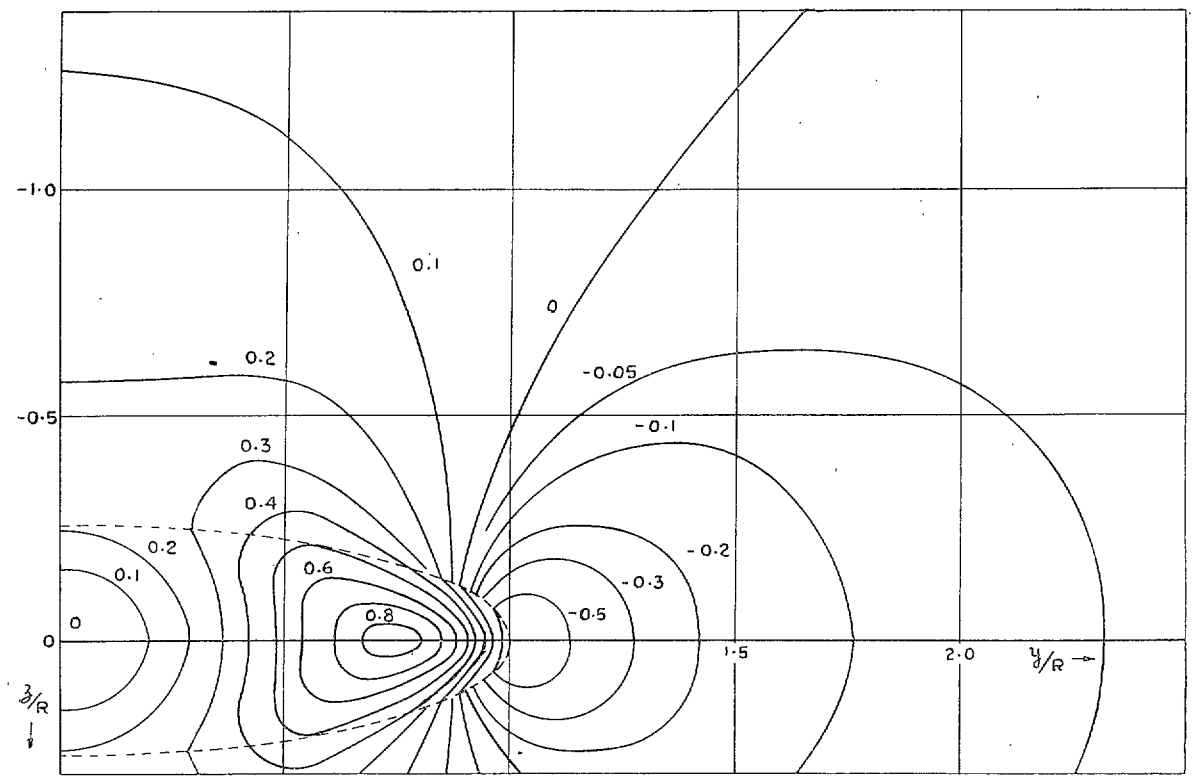

FIG. 18. Induced velocity far downstream for pressure distribution (III). Contours of w/VC_T for $i = 15$ deg.

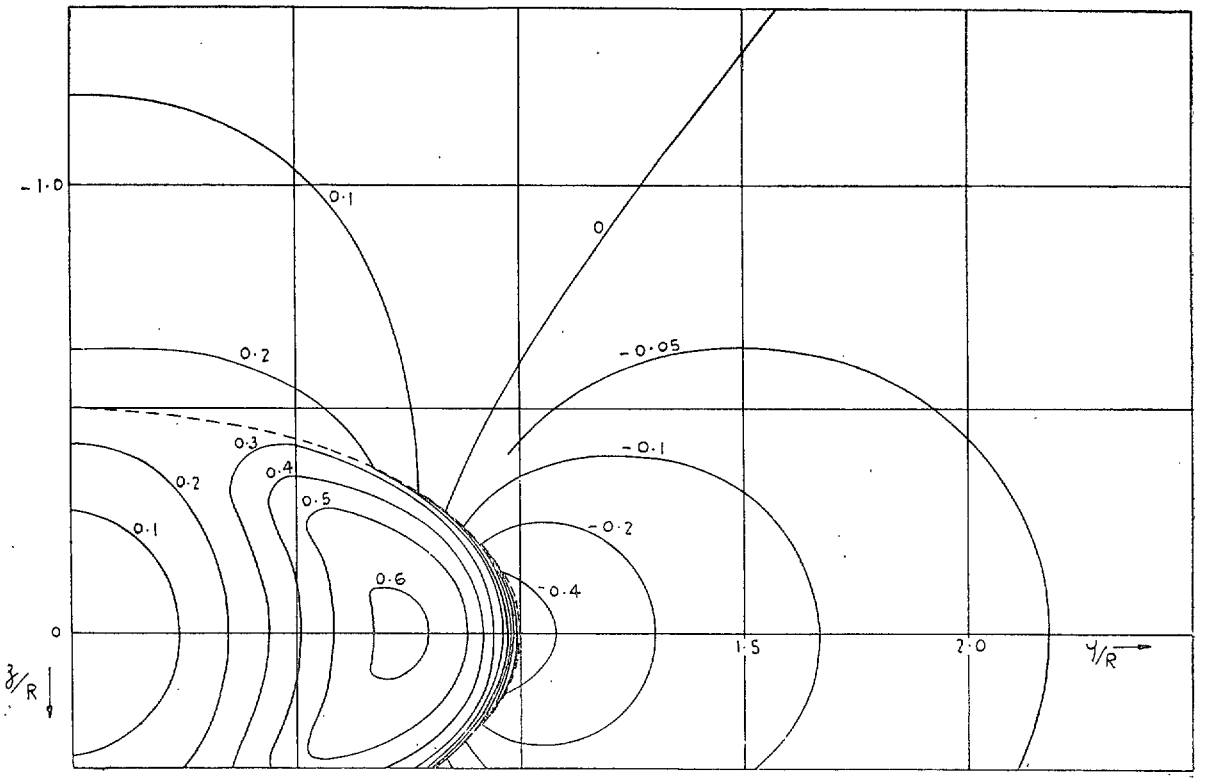

FIG. 19. Induced velocity far downstream for pressure distribution (III). Contours of w/VC_T for $i = 30$ deg.

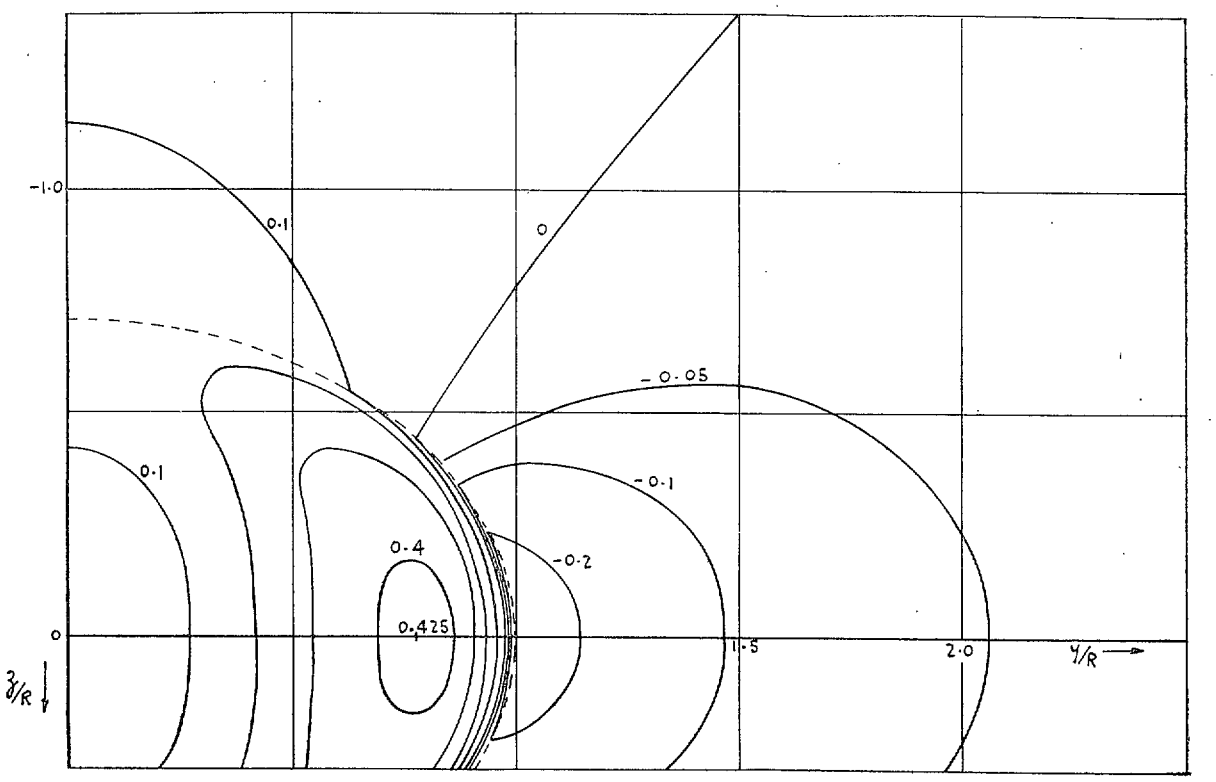

FIG. 20. Induced velocity far downstream for pressure distribution (III). Contours of w/VC_T for $i = 45$ deg.

J4286 Wt.15/680 K9 7/53 D&Co. 34/263

PRINTED IN GREAT BRITAIN

R. & M. No. 2642
(11,562 11,694)
A.R.C. Technical Report

Publications of the Aeronautical Research Council

ANNUAL TECHNICAL REPORTS OF THE AERONAUTICAL RESEARCH COUNCIL (BOUND VOLUMES)

1936 Vol. I. Aerodynamics General, Performance, Airscrews, Flutter and Spinning. 40*s.* (40*s.* 9*d.*)
Vol. II. Stability and Control, Structures, Seaplanes, Engines, etc. 50*s.* (50*s.* 10*d.*)

1937 Vol. I. Aerodynamics General, Performance, Airscrews, Flutter and Spinning. 40*s.* (40*s.* 10*d.*)
Vol. II. Stability and Control, Structures, Seaplanes, Engines, etc. 60*s.* (61*s.*)

1938 Vol. I. Aerodynamics General, Performance, Airscrews. 50*s.* (51*s.*)
Vol. II. Stability and Control, Flutter, Structures, Seaplanes, Wind Tunnels, Materials. 30*s.* (30*s.* 9*d.*)

1939 Vol. I. Aerodynamics General, Performance, Airscrews, Engines. 50*s.* (50*s.* 11*d.*)
Vol. II. Stability and Control, Flutter and Vibration, Instruments, Structures, Seaplanes, etc. 63*s.* (64*s.* 2*d.*)

1940 Aero and Hydrodynamics, Aerofoils, Airscrews, Engines, Flutter, Icing, Stability and Control, Structures, and a miscellaneous section. 50*s.* (51*s.*)

1941 Aero and Hydrodynamics, Aerofoils, Airscrews, Engines, Flutter, Stability and Control, Structures. 63*s.* (64*s.* 2*d.*)

1942 Vol. I. Aero and Hydrodynamics, Aerofoils, Airscrews, Engines. 75*s.* (76*s.* 3*d.*)
Vol. II. Noise, Parachutes, Stability and Control, Structures, Vibration, Wind Tunnels. 47*s.* 6*d.* (48*s.* 5*d.*)

1943 Vol. I. (*In the press.*)
Vol. II. (*In the press.*)

ANNUAL REPORTS OF THE AERONAUTICAL RESEARCH COUNCIL—

1933–34	1*s.* 6*d.* (1*s.* 8*d.*)	1937	2*s.* (2*s.* 2*d.*)
1934–35	1*s.* 6*d.* (1*s.* 8*d.*)	1938	1*s.* 6*d.* (1*s.* 8*d.*)
April 1, 1935 to Dec. 31, 1936.	4*s.* (4*s.* 4*d.*)	1939–48	3*s.* (3*s.* 2*d.*)

INDEX TO ALL REPORTS AND MEMORANDA PUBLISHED IN THE ANNUAL TECHNICAL REPORTS, AND SEPARATELY—

April, 1950 – – – – R. & M. No. 2600. 2*s.* 6*d.* (2*s.* 7½*d.*)

AUTHOR INDEX TO ALL REPORTS AND MEMORANDA OF THE AERONAUTICAL RESEARCH COUNCIL—

1909–1949 – – – – – R. & M. No. 2570. 15*s.* (15*s.* 3*d.*)

INDEXES TO THE TECHNICAL REPORTS OF THE AERONAUTICAL RESEARCH COUNCIL—

December 1, 1936 — June 30, 1939.	R. & M. No. 1850.	1*s.* 3*d.* (1*s.* 4½*d.*)
July 1, 1939 — June 30, 1945.	R. & M. No. 1950.	1*s.* (1*s.* 1½*d.*)
July 1, 1945 — June 30, 1946.	R. & M. No. 2050.	1*s.* (1*s.* 1½*d.*)
July 1, 1946 — December 31, 1946.	R. & M. No. 2150.	1*s.* 3*d.* (1*s.* 4½*d.*)
January 1, 1947 — June 30, 1947.	R. & M. No. 2250.	1*s.* 3*d.* (1*s.* 4½*d.*)
July, 1951 – – – –	R. & M. No. 2350.	1*s.* 9*d.* (1*s.* 10½*d.*)

Prices in brackets include postage.

Obtainable from

HER MAJESTY'S STATIONERY OFFICE

York House, Kingsway, London W.C.2 ; 423 Oxford Street, London W.1 (Post Orders : P.O. Box No. 569, London S.E.1) ; 13A Castle Street, Edinburgh 2 ; 39 King Street, Manchester 2 ; 2 Edmund Street, Birmingham 3 ; 1 St. Andrew's Crescent, Cardiff ; Tower Lane, Bristol 1 ; 80 Chichester Street, Belfast OR THROUGH ANY BOOKSELLER

S.O. Code No. 23-2642